THE JOURNAL OF BIOLOGICAL CHEMISTRY VOL. 283, NO. 18, pp. 12674–12679, May 2, 2008

Binding of Yeast Frataxin to the Scaffold for Fe-S Cluster Biogenesis, Isu*

Received for publication, January 16, 2008, and in revised form, February 27, 2008 Published, JBC Papers in Press, March 4, 2008, DOI 10.1074/jbc.M800399200

Tao Wang and Elizabeth A. Craig[1]

From the Department of Biochemistry, University of Wisconsin, Madison, Wisconsin 53706

Friedreich ataxia is caused by reduced activity of frataxin, a conserved iron-binding protein of the mitochondrial matrix, thought to supply iron for formation of Fe-S clusters on the scaffold protein Isu. Frataxin binds Isu in an iron-dependent manner *in vitro*. However, the biological relevance of this interaction and whether *in vivo* the interaction between frataxin and Isu is mediated by adaptor proteins is a matter of debate. Here, we report that alterations of conserved, surface-exposed residues of yeast frataxin, which have deleterious effects on cell growth, impair Fe-S cluster biogenesis and interaction with Isu while altering neither iron binding nor oligomerization. Our results support the idea that the surface of the β-sheet, adjacent to the acidic, iron binding ridge, is important for interaction of Yfh1 with the Fe-S cluster scaffold and point to a critical role for frataxin in Fe-S cluster biogenesis.

Friedreich ataxia (FRDA),[2] a progressive neurodegenerative disease, is caused by a decrease in the level, and in some cases activity, of frataxin, a highly conserved iron-binding protein of the mitochondrial matrix (1–3). The effects of deficiency of frataxin in human cells and Yfh1 in yeast are strikingly similar: decrease in the activity of Fe-S-containing enzymes and increase in intramitochondrial iron levels (4, 5). Not surprisingly considering their 65% amino acid identity, the tertiary structures of frataxin and Yfh1 are very similar, a β-sheet packed against two α-helices (6–8). The larger helix and part of the adjacent β-strand form an acidic ridge that binds iron. While a Yfh1 monomer can bind 2 ferrous irons (8, 9), it also undergoes iron-dependent oligomerization to form trimers and ultimately oligomers having up to 48 subunits that bind >2000 iron atoms (10, 11). Alterations in the acidic residues of the ridge can affect oligomerization and thus robust iron binding, alleviating any ability to serve an iron storage function (12, 13).

Evidence indicates that Yfh1/frataxin plays an important role in the formation of Fe-S clusters (5, 14) on the highly conserved scaffold Isu prior to transfer to recipient apoproteins (15). Its proposed role as an iron donor is supported by its high affinity, iron-dependent interaction with Isu and its ability to donate iron for cluster formation on Isu *in vitro* (16). In addition, evidence strongly indicates that Nfs1, an essential cysteine desulfurase, which is required for Fe-S cluster formation on Isu *in vivo*, functions as the sulfur donor (17, 18). Another essential protein, Isd11, is also required for *in vivo* Fe-S cluster formation (15, 19). It forms a stable complex with Nfs1 and is required for Nfs1 to be stable *in vivo*.

The manner in which the activities of these proteins, including their physical interactions, are coordinated to allow cluster formation on Isu *in vivo* is a matter of debate. Most relevant to this report, it has been recently argued that the relevant *in vivo* interaction between frataxin homologs and scaffolds is indirect, despite the fact that an interaction has been observed *in vitro* (16). In human cells data indicate that the interaction is mediated by Isd11 (20). In the case of bacteria, which do not have an Isd11 homolog, the available data indicate that the cysteine desulfurase Nfs1, the ortholog of eukaryotic IscS, is necessary for the interaction (21).

One of the roadblocks to a better understanding of the nature of the Yfh1-Isu interactions has been its iron dependence. To date, the only *YFH1* mutations found to render cells defective in Fe-S cluster biogenesis are thought to affect iron binding (22), making it difficult to separate effects caused by defects in iron binding *per se* from those affecting the Isu-Yfh1 interaction itself. Therefore, we sought mutations in *YFH1* that altered interaction with Isu, but not iron binding. We found that alterations of conserved residues 122–124 of the β-sheet preserve normal iron binding and oligomerization capacity but compromise interaction with Isu.

EXPERIMENTAL PROCEDURES

Strains and Plasmids—Saccharomyces cerevisiae strains carrying *YFH1* genes on plasmids were created by sporulation and dissection of *YFH1/yfh1*Δ or *YFH1/yfh1*Δ *ISU1/isu1*Δ (W303 background) transformed with the plasmids. *YFH1* mutants were generated by site-directed mutagenesis using pCM189-YFH1 (12), having *YFH1* under the control of the tetO promoter, as template. *yfh1*Δ with tetO-$yfh1_{86/90/93A}$ integrated at the *LEU2* locus was used to prepare extracts for pulldown assays (12). For increased expression, *ISU1*, *NFS1*, and *ISD11* were expressed under the control of the *GAL4* promoter in a high copy vector (pYES2) in minimal medium. Doxycycline was used at 1 μg/ml.

Assays—Protein purification and oligomerization assays were performed by size exclusion chromatography essentially as described (12) after incubating Yfh1 (5 μM) with

* This work was supported by the Muscular Dystrophy Association, National Institutes of Health Grant GM27870 (to E. A. C.), and American Heart Association Postdoctoral Fellowship 0525728Z (to T. W.). The costs of publication of this article were defrayed in part by the payment of page charges. This article must therefore be hereby marked "*advertisement*" in accordance with 18 U.S.C. Section 1734 solely to indicate this fact.

[1] To whom correspondence should be addressed: Dept. of Biochemistry, 433 Babcock Dr., University of Wisconsin, Madison, WI 53706-1544. Tel.: 608-263-7105; Fax: 608-262-3453; E-mail: ecraig@wisc.edu.

[2] The abbreviations used are: FRDA, Friedreich ataxia; WT, wild type; Ni-NTA, nickel-nitrilotriacetic acid.

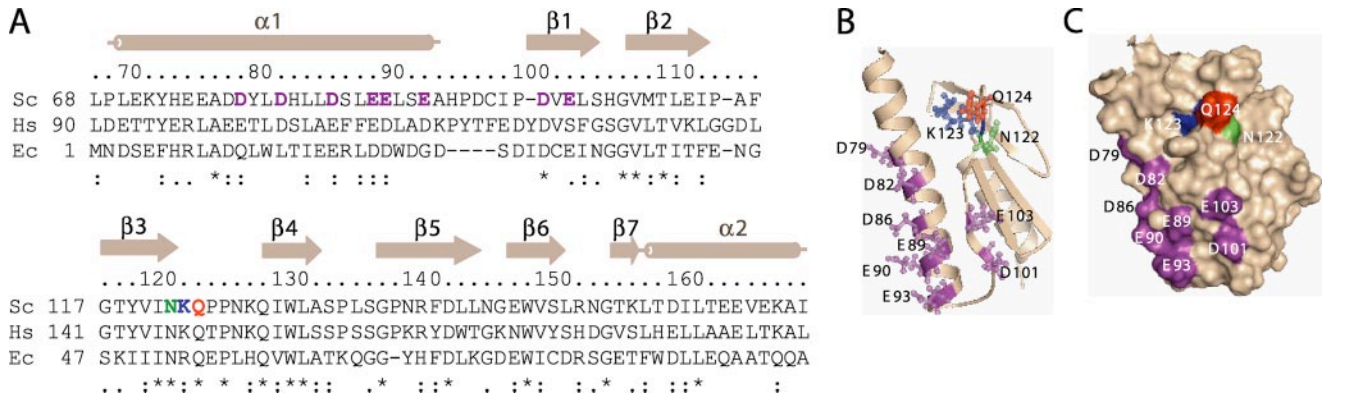

FIGURE 1. **Yfh1 structure.** *A*, ClustalX alignment of sequences corresponding to the α1-α2 region of Yfh1. *S. cerevisiae*, Yfh1 (*Sc*); *Homo sapiens*, frataxin (*Hs*); *Escherichia coli*, CyaY (*Ec*). Secondary structural elements and numbering referring to Yfh1 are above the sequences. Iron binding residues from Ref. 9 (*purple*), Asn-122 (*green*), Lys-123 (*blue*), Gln-124 (*red*) are indicated. Identical (*) and highly similar (:) residues are indicated. Ribbon (*B*) and space-filled Yfh1 (Protein Data Bank accession code 2ga5) (*C*), generated using PyMOL (29). Color coding as in *A*. The N-terminal residues (52–67) are not shown.

$Fe(NH_4)_2(SO_4)_2$ at indicated molar ratios. To assess iron binding, half of the sample was applied to a 0.5-ml ultrafree centrifugal filter (cut off of 5 kDa; Millipore) and centrifuged at 12,000 × *g* for ~8 min. Iron in the retenate was determined photospectroscopically by measuring the amount of Fe[2,2′-bipyridine]$_3^{2+}$ formed (23).

Pulldown assays using mitochondrial lysates were performed as described previously with minor modifications (12). 500 μg of mitochondria was lysed by incubation for 15 min on ice in 500 μl of 50 mM Tris-HCl, pH 7.5, buffer containing 80 mM KCl, 0.1% Triton X-100, 50 μM pyridoxal phosphate, 1 mM ascorbic acid, 10 mM imidazole, 50 μM $Fe(NH_4)_2(SO_4)_2$, and complete EDTA-free protein inhibitor mixture (Roche Applied Science). Membrane debris was removed by centrifugation at 16,000 × *g* for 10 min at 4 °C. 4 μg of His-tagged wild type (WT) or mutant Yfh1 was added into the supernatant and incubated for 1 h at 4 °C. Bovine serum albumin was added in place of Yfh1 for control reactions. 15 μl of His-tagged resin (~7.5 μl bead volume) was then added to the reaction mixture and incubation continued for an additional hour at 4 °C. Beads were collected by centrifugation and washed three times with 500 μl of lysis buffer without Triton X-100 and with 60 mM imidazole. After the final wash, sample buffer was added to the reaction mixtures, and after a short spin all of the supernatant was loaded on a SDS-polyacrylamide gel. Proteins bound to the beads were analyzed by immunoblot analysis using appropriate antibodies.

Pulldown assays using purified recombinant Yfh1 and Isu1 proteins were performed by incubating indicated concentrations of Isu1 (24) and iron-loaded Yfh1 proteins in 100 μl of buffer for 45 min at room temperature (20 mM Tris-HCl, pH 7.5, 125 mM KCl, 1 mM ascorbic acid, 50 μM $Fe(NH_4)_2(SO_4)_2$, 0.05% (v/v) Triton X-100, 50 mM imidazole). Yfh1 proteins were preincubated with $Fe(NH_4)_2(SO_4)_2$ for 1 h at 30 °C. Ni-NTA-agarose beads were equilibrated with lysis buffer and preincubated with 0.1% bovine serum albumin. 15 μl of beads (~7.5 μl bead volume) were added to each reaction, and the mixture was incubated at 4 °C for 1 h with rotation. The beads were washed four times with 500 μl of buffer, and proteins bound to the beads were loaded on a SDS-polyacrylamide gel and incubated with SYPRO-Ruby protein stain (Molecular Probes, Eugene, OR) to allow quantitation of protein. All measurements for aconitase, succinate dehydrogenase and iron (25), and citrate synthase (26) were performed as described, using mitochondria prepared from cells grown in minimal glucose medium in the presence or absence of doxycycline.

RESULTS

Alteration of Residues in the β-Strand 3–4 Region—Because our goal was identification of residues important for iron-independent interaction between Yfh1 and Isu, we searched for highly conserved, surface-exposed residues outside the acid ridge formed by α-helix 1 and a portion of β-strand 1 that is predicted from NMR spectroscopy studies to directly interact with iron atoms (9). We decided to focus on three adjacent residues at the end of β-strand 3 and the beginning of the loop leading to β-strand 4, Asn-122, Lys-123, and Gln-124. Asn-122 and Gln-124 are surface-exposed and invariant among known frataxin homologs (Fig. 1). Lys-123 is also well conserved, being either lysine or arginine, except in *Rickettsia prowazekii*, which has a threonine at this position. Lys-123 is partially accessible to solution.

Codons Asn-122, Lys-123, and Gln-124 were mutated to encode alanine, threonine and alanine, respectively, both singly and in combination. The mutant genes were placed under the control of the tetO promoter to allow modulation of expression. As expected (12), in the absence of doxycycline WT Yfh1 was expressed at levels similar to that found when expressed from its own promoter, and the mutant strains grew like WT even in the presence of drug when expression was reduced ~10-fold (Fig. 2*A*). All mutants also grew as well as WT in the absence of drug. However, in the presence of drug, growth of $yfh1_{K123T}$ and the triple mutant $yfh_{N122A/K123T/Q124A}$, hereafter called $yfh1_{122-4}$, was significantly affected. To determine whether this poor growth was simply due to decreased expression, cell extracts were subjected to immunoblot analysis using Yfh1-specific antibody (Fig. 2*B*). $Yfh1_{K123T}$ was expressed at much lower levels than WT Yfh1. However, $Yfh1_{122-4}$ was expressed at levels comparable with WT in both the presence and absence of drug. We therefore concentrated our efforts on $yfh1_{122-4}$.

Lowered Mitochondrial Fe-S Enzyme Activity of yfh_{122-4}—Because an accumulation of mitochondrial iron and a decrease

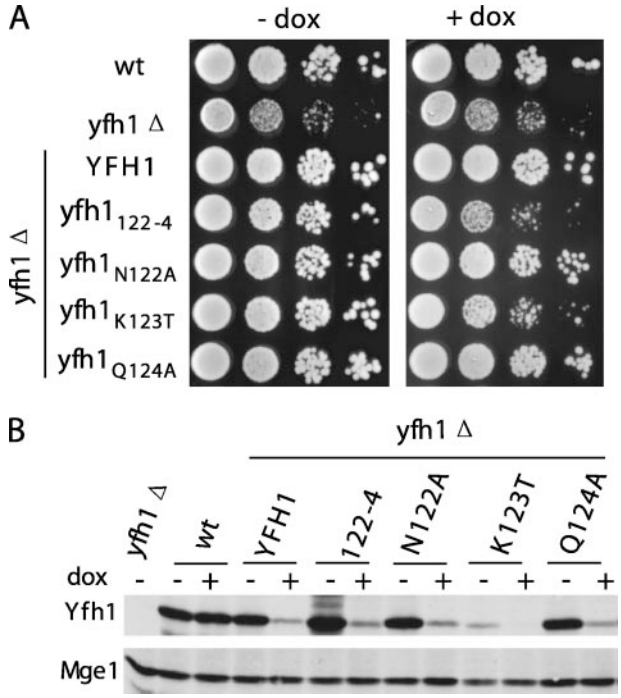

FIGURE 2. **Growth of *YFH1* mutants.** *A*, 10-fold serial dilutions of cell suspensions of WT, *yfh1*Δ, and *yfh1*Δ transformed with plasmids carrying the indicated tetO-regulatable WT or mutant *YFH1* were plated on rich glucose medium containing (+) or lacking (−) doxycycline (*dox*). *yfh*$_{N122A/K123T/Q124A}$, (*yfh1*$_{122-4}$). Plates were incubated at 30 °C for 2 days. *B*, cells grown as in *A* were harvested and subjected to SDS-PAGE followed by immunoblot analysis using Yfh1 and, as a loading control, Mge1-specific antibodies.

in activity of Fe-S enzymes is a hallmark of Yfh1 deficiency (15), mitochondria were isolated from WT and yfh1$_{122-4}$ cells grown in the presence or absence of drug. Iron concentration and activities of two Fe-S enzymes, aconitase and succinate dehydrogenase, as well as a control enzyme lacking an Fe-S cluster, citrate synthase, were measured (Table 1). Even under normal Yfh1 expression levels, conditions under which no growth difference was observed (Fig. 2*A*), mutant mitochondria had nearly 2-fold higher iron levels and less than half the aconitase and succinate dehydrogenase activity of WT (Table 1). When expression of Yfh1 was lowered, WT mitochondrial iron increased only ~50% and the aconitase and succinate dehydrogenase activities decreased on the order of 30%. In contrast, in the mutant, iron accumulated an additional 3-fold and aconitase and succinate dehydrogenase activities were dramatically reduced, to ~5 and 15%, respectively, of that normally present in WT. Citrate synthase activity was unaffected regardless of Yfh1 expression levels. We conclude that Yfh1$_{122-4}$ is less active than WT Yfh1.

Yfh1$_{122-4}$ Binds Iron and Oligomerizes Normally—Next, we compared the iron binding properties of WT Yfh1 and Yfh1$_{122-4}$. Purified proteins were incubated in the presence of varying amounts of iron prior to separation of bound and free iron by filtration. Yfh1$_{122-4}$ bound iron as efficiently as WT protein at all iron concentrations tested, up to ~20 atoms/monomer at a Yfh1:iron ratio of 1:30 (Fig. 3*A*). As a control, we tested the oligomerization-deficient Yfh1$_{86/90/93A}$, having Asp-86, Glu-90, and Glu-93 changed to alanine (12). Regardless of

TABLE 1
Mitochondrial iron content and respiratory enzyme activities
SDH, succinate dehydrogenase.

Gene under tetO	Doxycycline	Iron[a,b]	Aconitase[a,c]	SDH[a,c]	Citrate synthase[a,c]
YFH1	−	5.8 ± 1.6	1166 ± 260	32.6 ± 8	180 ± 5
yfh1$_{122-4}$	−	10.5 ± 2[d]	497 ± 73[d]	14.8 ± 3.7[d]	270 ± 10
YFH1	+	8.8 ± 1.3	774 ± 152	22.1 ± 5.6	210 ± 4
yfh1$_{122-4}$	+	30.1 ± 1[d,e]	68 ± 5[d,e]	4.7 ± 1.1[d,e]	250 ± 7

[a] Values obtained are an average of at least three independent mitochondrial preparations; ± indicates range observed.
[b] Iron content as nmol/mg of mitochondrial protein.
[c] Enzyme activities are defined as 1 nmol substrate converted/min/mg of mitochondrial protein.
[d] Indicates significant difference from *YFH1* under the same growth conditions ($p < 0.01$).
[e] Indicates significant difference from *yfh1$_{122-4}$* in the absence of doxycycline ($p < 0.01$).

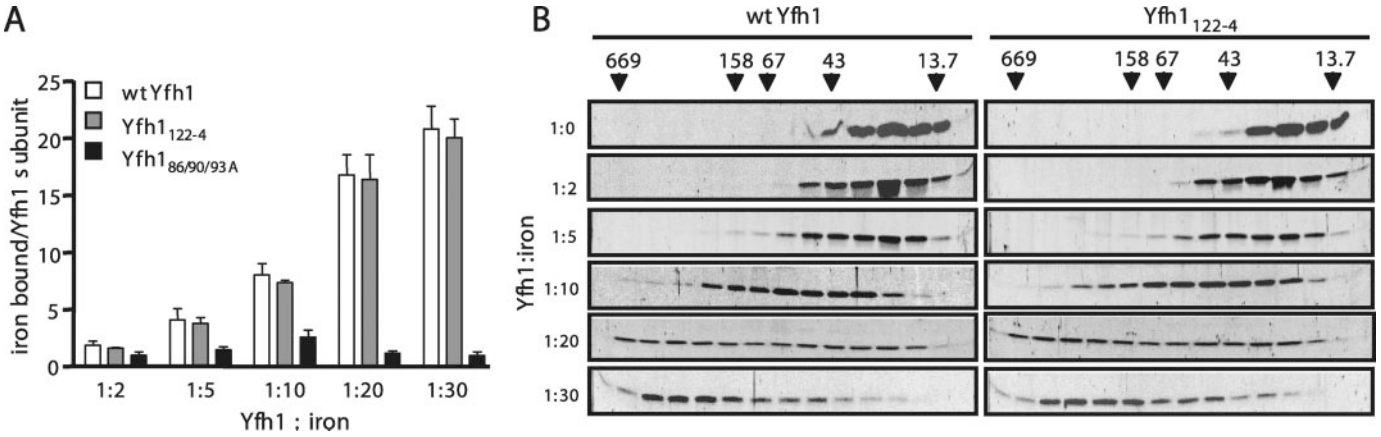

FIGURE 3. **Iron binding and oligomerization.** *A*, purified Yfh1 proteins were incubated with ferrous iron at the indicated protein to iron ratios and then split into two equal parts and subjected to iron quantitation spectroscopically (see "Experimental Procedures" for details). *Bars* represent the means ± S.E. of at least three independent reactions. *B*, gel filtration chromatography. Fractions were resolved by SDS-PAGE and stained with SYPRO-Ruby. Positions of thymoglobulin (*669 kDa*), aldolase (*158 kDa*), bovine serum albumin (*67 kDa*), ovalbumin (*43 kDa*), and ribonuclease A (*13.7 kDa*) are indicated.

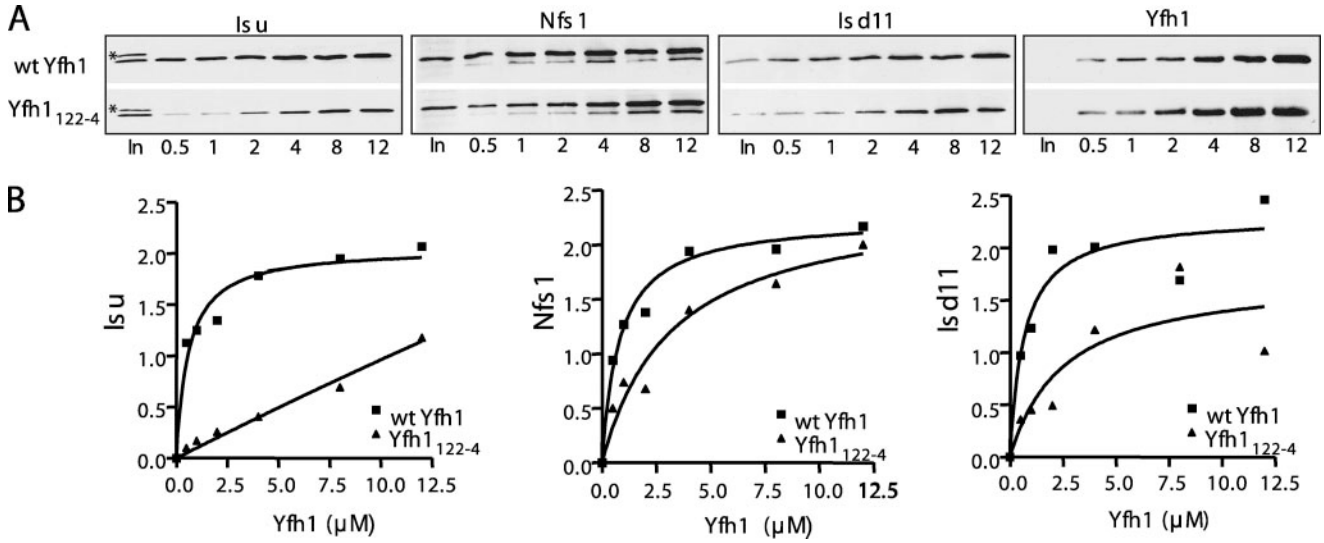

FIGURE 4. **Interaction with Isu and other Fe-S cluster assembly proteins in mitochondria extracts.** *A*, indicated concentrations of His-tagged Yfh1 or Yfh_{122-4} were incubated with a mitochondrial extract. Proteins pulled down by Ni-NTA resins were detected by immunoblot using antibodies against indicated proteins after resolution by SDS-PAGE. *Left lane*, 5% of total input (*In*). Similar experiments were done a minimum of three times; a representative experiment is shown. The band indicated by the asterisk (*) is a cross-reacting protein, unrelated to Isu. *B*, immunoblot signals were quantitated by densitometry and plotted against Yfh1 protein concentrations. 5% input was set as 1. All curves were plotted in Prism using a single binding hyperbola to fit data, except that Isu/Yfh_{122-4} was fitted by linear regression.

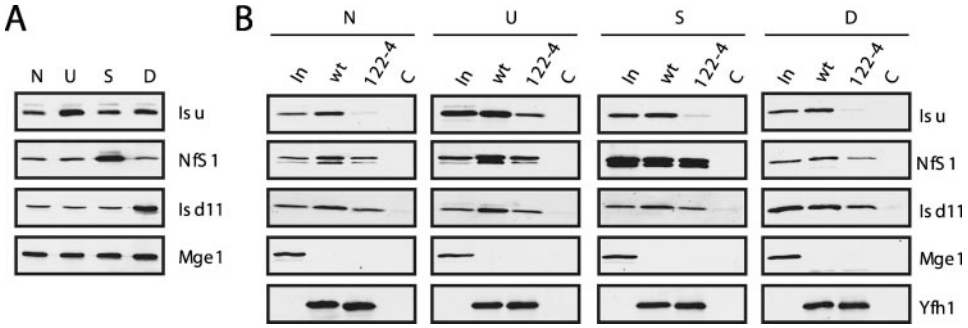

FIGURE 5. **Yfh1 interaction with Isu and Isd11/Nfs1 in mitochondria extracts with up-regulated expression level of Isu, Ids11, or Nfs1.** *A*, expression level of Isu, Nfs1, and Isd11 in mitochondrial samples. *N*, normal expression; overexpression of Isu1 (*U*), Nfs1 (*S*), Isd11 (*D*). Mge1 serves as a loading control. *B*, purified His-tagged WT Yfh1 or Yfh_{122-4} (final concentration of ~0.5 μM) was added to the indicated mitochondrial extracts. Protein complexes pulled down by Ni-NTA resin were analyzed by immunoblot analysis using antibodies against the indicated proteins. Mge1 serves as a negative control. 5% input (*In*); WT Yfh1 (*WT*), $Yfh1_{122-4}$ (*122–4*), control, no Yfh1 proteins were added to the reactions (*C*).

the iron concentration used, $Yfh1_{86/90/93A}$ bound ~2 iron atoms/subunit, consistent with the capacity of monomeric Yfh1 (9).

Oligomerization was tested directly by gel filtration chromatography. As previously reported (12), WT Yfh1 formed sequentially larger homo-oligomers as iron concentration increased (Fig. 3*B*), while $Yfh1_{86/90/93A}$ was eluted at the monomer position in the presence and absence of iron (Fig. 3*B*, data not shown). The pattern of $Yfh1_{122-4}$ elution was similar to that of WT Yfh1. At a 1:30 ratio of protein to iron, negligible amounts of Yfh1 and $Yfh1_{122-4}$ remained as monomers. Taken together, our data indicate that $Yfh1_{122-4}$ is defective in neither iron binding nor oligomerization.

Defect in $Yfh1_{122-4}$-Isu Interaction in Extracts—Because iron binding and iron-induced oligomerization of $Yfh1_{122-4}$ appeared normal but mitochondria expressing this form of Yfh1 had low Fe-S cluster enzyme activity, we asked whether interaction with the scaffold Isu or other proteins involved in cluster formation was affected. Purified His-tagged Yfh1, at concentrations from ~0.5 to 12 μM, were incubated with mitochondrial extracts and then with Ni-NTA resin to "pull down" Yfh1 and proteins bound to it. To avoid potential problems due to the presence of oligomerization-competent Yfh1, lysates were prepared from cells expressing $Yfh1_{86/90/93A}$ at low levels. Isu association with Yfh1 was saturable, with 50% binding being reached at ~1 μM (Fig. 4). The affinity of Isu for $Yfh1_{122-4}$ was much lower. Saturation was not reached; at 12 μM $Yfh1_{122-4}$ at about the same amount of Isu was pulled down as at 0.5–1 μM Yfh1. As expected, this residual binding was iron-dependent (data not shown). Interaction between Yfh1 and Nfs1, as well as Isd11, was also monitored, as recent results implicated Isd11 as a possible direct Yfh1 interaction partner in human cells (20). Interaction between Yfh1 and Nfs1/Isd11 was also affected by alterations in 122–124, but to a lesser extent than Isu. In particular, Nfs1 interaction was only modestly affected.

In light of the proposed adaptor roles of Nfs1 and Isd11, we also tested the effect of higher concentrations of individual components on Isu binding to $Yfh1_{122-4}$. His-tagged WT or mutant Yfh1 (0.5 μM) was incubated with lysates from mitochondria having increased expression of Isu, Nfs1, or Isd11 (Fig. 5*A*). As expected, when Isu levels were increased, more of the overexpressed Isu was pulled down (Fig. 5*B*). When Nfs1 or Isd11 levels were higher, more of the protein whose expression was elevated co-eluted with both mutant and WT Yfh1. However, no increase in interaction of Isu with either WT or mutant Yfh1 was observed.

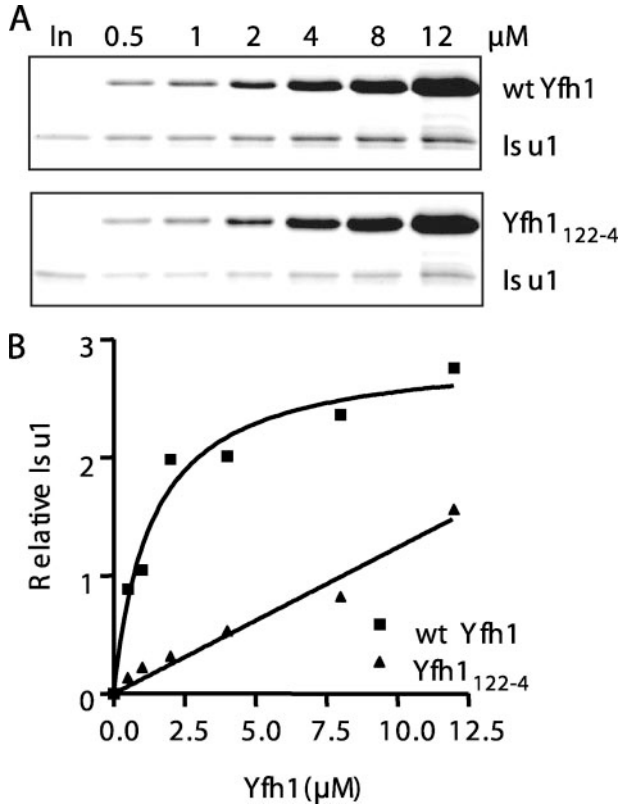

FIGURE 6. **Interaction of purified Yfh1 and Isu1.** *A*, 5 μM Isu1 and His-tagged Yfh1 or Yfh_{122-4} at the concentrations indicated were preincubated to allow complex formation. Ni-NTA resins were added to pull down the complexes that were analyzed by SDS-PAGE and SYPRO-Ruby staining. *Leftmost lane*, 20% Isu1 input. *B*, bound Isu1 was quantitated by densitometry. 20% input Isu1 was set as 1. Values were plotted in Prism using a single binding hyperbola to fit data obtained for wild type Yfh1 and linear regression to fit Yfh_{122-4} data.

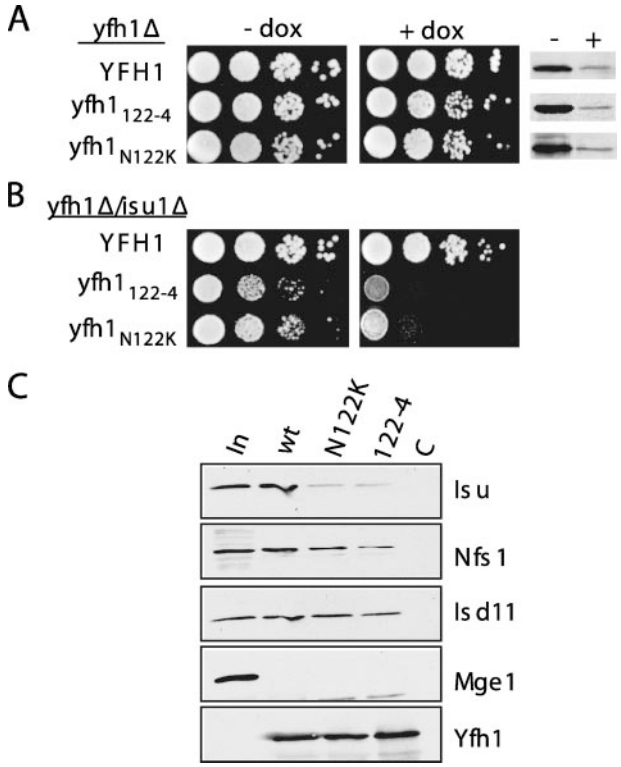

FIGURE 7. **Characterization of FRDA-associated $yfh1_{N122K}$.** *A* and *B*, 10-fold serial dilutions of *yfh1*Δ (*A*) or *yfh1*Δ/*isu1*Δ (*B*) transformed with plasmids carrying tetO-regulatable *YFH1*, $yfh1_{N122K}$, or $yfh1_{122-4}$ were spotted on rich glucose medium containing (+) or lacking (−) doxycycline and incubated at 30 °C for 2 days. *A*, *right panel*, immunoblot analysis of lysates from plates using Yfh1-specific antibody. *C*, $Yfh1_{N122K}$ interaction with Isu and other Fe-S cluster assembly proteins in mitochondria extracts. Indicated His-tagged Yfh1 were incubated with mitochondrial extract; proteins pulled down by Ni-NTA resins were detected using antibodies against the indicated proteins after SDS-PAGE. 5% of input (*In*); control, no Yfh1 protein added to reactions (*C*).

Defect in $Yfh1_{122-4}$-Isu Interaction in Vitro—The results of assays using mitochondrial lysates are consistent with the idea that alterations in residues 122–124 directly affect Isu binding. To test this idea, we developed a pulldown assay using only purified components. Similar to the titration using mitochondrial extracts, different amounts of His-Yfh1 protein were incubated with Isu1. Yfh1 along with any associated Isu was pulled down using Ni-NTA resin (Fig. 6). The binding curve for Yfh1 was saturable. $Yfh1_{122-4}$ displayed a significantly reduced affinity for Isu, failing to reach saturation under the conditions used.

FRDA-associated $Yfh1_{N122K}$ Is Defective in Interaction with Isu—The point mutation N146K has been identified in one FRDA patient (27). We constructed the corresponding mutation in *YFH1*, $yfh1_{N122K}$. When expressed at normal levels, $Yfh1_{N122K}$ fully rescued the growth of *yfh1*Δ. $yfh1_{N122K}$ grew somewhat more slowly than WT when expression was reduced by addition of drug (Fig. 7*A* and data not shown), indicating a partial loss of function. As a second *in vivo* test, we took advantage of the fact that cells lacking both Yfh1 and Isu1, one of the two closely related Isu scaffolds, are inviable (28), although low levels of Yfh1 are sufficient to maintain robust growth (12) (Fig. 7*B*). However, neither $Yfh1_{N122K}$ nor $Yfh1_{122-4}$ was able to significantly overcome the deleterious effect of the reduced level of Isu.

The interaction of $Yfh1_{N122K}$ with proteins in mitochondrial extracts was also tested (Fig. 7*C*). Significantly less Isu was pulled down from extracts by $Yfh1_{N122K}$ than by WT Yfh1; on the other hand, only slightly less Isd11 and Nfs1 were retained. Thus, the change at position 122 to lysine disrupts both *in vivo* function and interaction with Isu.

DISCUSSION

Our data support the idea that residues at the end of β-strand 3 are important for the direct interaction of Yfh1 with Isu. $Yfh1_{122-4}$ shows reduced interaction with Isu, not only when in the complex milieu of mitochondrial extracts but also in the absence of other proteins. We propose that the defect in interaction with Isu is not attributable to defective iron binding but rather to deleterious effects on direct protein-protein contacts. Not only did WT and mutant Yfh1 bind iron and oligomerize similarly, residues 122–124 did not show amide line broadening upon iron binding in NMR spectroscopy studies (9). Such broadening would not be expected, because these residues 122–124 are neither acidic themselves nor in extremely close proximity to acidic residues, the presumed iron binding ligands. However, the residues 122–124 identified in our study are physically in close proximity to the acidic ridge. It is likely that *in vivo* interaction of Yfh1 with Isu involves both iron-protein and protein-protein contacts.

Although our results are not consistent with the simple scenario that either Nfs1 or Isd11 serves as an exclusive adapter for the interaction of Yfh1 with Isu, we do not mean to imply that interaction between Yfh1 and Isu is unaffected by other proteins. A complex choreography of protein-protein interactions must occur to foster both Fe-S cluster formation on and transfer from Isu. Indeed, the association of Isd11 in mitochondrial extracts with $Yfh1_{122-4}$ was also affected. Testing of a direct interaction between the two proteins awaits purification of Isd11. It is perhaps most likely that a complex picture will emerge at that point, with each component interacting with several partners, perhaps simultaneously, rather than a simple bidirectional set of protein-protein interactions such as Yfh1 interacting only with Isu or only with Isd11/Nfs1.

Most identified missense mutations that cause FRDA affect the stability of frataxin, not surprisingly, because they alter residues in the interior hydrophobic core of the protein. The identification of a surface-exposed alteration at the end of β-strand 3 as a cause of FRDA, coupled with the results reported here, lends credence not only to the functional importance of this region but also to the idea that the primary function of frataxin is to facilitate efficient Fe-S cluster biogenesis.

Acknowledgments—We thank Klaus Pfanner and Andrew Dancis for providing antibodies against Ids11 and Nfs1, respectively, and Roland Lill for pYES2-Nfs1.

REFERENCES

1. Campuzano, V., Montermini, L., Molto, M. D., Pianese, L., Cossee, M., Cavalcanti, F., Monros, E., Rodius, F., Duclos, F., Monticelli, A., Zara, F., Canizares, J., Koutnikova, H., Bidichandani, S. I., Gellera, C., Brice, A., Trouillas, P., De Michele, G., Filla, A., De Frutos, R., Palau, F., Patel, P. I., Di Donato, S., Mandel, J. L., Cocozza, S., Koenig, M., and Pandolfo, M. (1996) *Science* **271,** 1423–1427
2. Cossee, M., Durr, A., Schmitt, M., Dahl, N., Trouillas, P., Allinson, P., Kostrzewa, M., Nivelon-Chevallier, A., Gustavson, K. H., Kohlschutter, A., Muller, U., Mandel, J. L., Brice, A., Koenig, M., Cavalcanti, F., Tammaro, A., De Michele, G., Filla, A., Cocozza, S., Labuda, M., Montermini, L., Poirier, J., and Pandolfo, M. (1999) *Ann. Neurol.* **45,** 200–206
3. Puccio, H., and Koenig, M. (2000) *Hum. Mol. Genet.* **9,** 887–892
4. Babcock, M., de Silva, D., Oaks, R., Davis-Kaplan, S., Jiralerspong, S., Montermini, L., Pandolfo, M., and Kaplan, J. (1997) *Science* **276,** 1709–1712
5. Rotig, A., de Lonlay, P., Chretien, D., Foury, F., Koenig, M., Sidi, D., Munnich, A., and Rustin, P. (1997) *Nat. Genet.* **17,** 215–217
6. Dhe-Paganon, S., Shigeta, R., Chi, Y. I., Ristow, M., and Shoelson, S. E. (2000) *J. Biol. Chem.* **275,** 30753–30756
7. He, Y., Alam, S. L., Proteasa, S. V., Zhang, Y., Lesuisse, E., Dancis, A., and Stemmler, T. L. (2004) *Biochemistry* **43,** 16254–16262
8. Bencze, K. Z., Kondapalli, K. C., Cook, J. D., McMahon, S., Millan-Pacheco, C., Pastor, N., and Stemmler, T. L. (2006) *Crit. Rev. Biochem. Mol. Biol.* **41,** 269–291
9. Cook, J. D., Bencze, K. Z., Jankovic, A. D., Crater, A. K., Busch, C. N., Bradley, P. B., Stemmler, A. J., Spaller, M. R., and Stemmler, T. L. (2006) *Biochemistry* **45,** 7767–7777
10. Park, S., Gakh, O., O'Neill, H. A., Mangravita, A., Nichol, H., Ferreira, G. C., and Isaya, G. (2003) *J. Biol. Chem.* **278,** 31340–31351
11. Cavadini, P., O'Neill, H. A., Benada, O., and Isaya, G. (2002) *Hum. Mol. Genet.* **11,** 217–227
12. Aloria, K., Schilke, B., Andrew, A., and Craig, E. A. (2004) *EMBO Rep.* **5,** 1096–1101
13. Gakh, O., Park, S., Liu, G., Macomber, L., Imlay, J. A., Ferreira, G. C., and Isaya, G. (2006) *Hum. Mol. Genet.* **15,** 467–479
14. Muhlenhoff, U., Richhardt, N., Ristow, M., Kispal, G., and Lill, R. (2002) *Hum. Mol. Genet.* **11,** 2025–2036
15. Wiedemann, N., Urzica, E., Guiard, B., Muller, H., Lohaus, C., Meyer, H. E., Ryan, M. T., Meisinger, C., Muhlenhoff, U., Lill, R., and Pfanner, N. (2006) *EMBO J.* **25,** 184–195
16. Yoon, T., and Cowan, J. A. (2003) *J. Am. Chem. Soc.* **125,** 6078–6084
17. Zheng, L., White, R. H., Cash, V. L., Jack, R. F., and Dean, D. R. (1993) *Proc. Natl. Acad. Sci. U. S. A.* **90,** 2754–2758
18. Muhlenhoff, U., Balk, J., Richhardt, N., Kaiser, J. T., Sipos, K., Kispal, G., and Lill, R. (2004) *J. Biol. Chem.* **279,** 36906–36915
19. Adam, A. C., Bornhovd, C., Prokisch, H., Neupert, W., and Hell, K. (2006) *EMBO J.* **25,** 174–183
20. Shan, Y., Napoli, E., and Cortopassi, G. (2007) *Hum. Mol. Genet.* **16,** 929–941
21. Layer, G., Ollagnier-de Choudens, S., Sanakis, Y., and Fontecave, M. (2006) *J. Biol. Chem.* **281,** 16256–16263
22. Foury, F., Pastore, A., and Trincal, M. (2007) *EMBO Rep.* **8,** 194–199
23. O'Neill, H. A., Gakh, O., Park, S., Cui, J., Mooney, S. M., Sampson, M., Ferreira, G. C., and Isaya, G. (2005) *Biochemistry* **44,** 537–545
24. Andrew, A. J., Dutkiewicz, R., Knieszner, H., Craig, E. A., and Marszalek, J. (2006) *J. Biol. Chem.* **281,** 14580–14587
25. Voisine, C., Cheng, Y. C., Ohlson, M., Schilke, B., Hoff, K., Beinert, H., Marszalek, J., and Craig, E. A. (2001) *Proc. Natl. Acad. Sci. U. S. A.* **98,** 1483–1488
26. Parvin, R. (1969) *Methods Enzymol.* **13,** 16–19
27. Zühlke, C. H., Dalski, A., Habeck, M., Straube, K., Hedrich, K., Hoeltzenbein, M., Konstanzer, A., Hellenbroich, Y., and Schwinger, E. (2004) *Eur. J. Hum. Genet.* **11,** 979–982
28. Ramazzotti, A., Vanmansart, V., and Foury, F. (2004) *FEBS Lett.* **557,** 215–220
29. DeLano, W. L. (2002) The PyMOL Molecular Graphics System, DeLano Scientific LLC, San Carlos, CA